New Methodologies for the Preparation of Porphodimethenes and Their Conversion to *trans*-Porphyrins with Functionalized Naphthyl Spacers

Michael Harmjanz, Hubert S. Gill, and Michael J. Scott*

Department of Chemistry, University of Florida, P.O. Box 117200, Gainesville, Florida 32611-7200

mjscott@chem.ufl.edu

Received February 12, 2001

The MacDonald [2 + 2]-type condensation of readily available 5-aryl-substituted dipyrromethanes with acenaphthenequinone leads to the *trans-syn*- and *anti*-porphodimethenes, which in turn can be converted to the α,α- and α,*β*-porphyrin atropisomers, respectively. Treatment of the metalated or unmetalated porphodimethenes with KOH or NaOMe in THF followed by protonation with HCl results in a ring opening of the acenaphthenone and formation of the *trans*-8-carboxynaphthylporphyrins or their esters (NaOMe) after oxidation. Alternatively, the porphyrin formation can be accomplished by reaction of the porphodimethenes with acids in the presence of water or methanol. Reaction with $NaBH_4$ in a THF−methanol mixture yields the corresponding dialcohols in nearly quantitative yields. Sixteen different building blocks were prepared in order to evaluate the generality of this new synthetic approach, with Ar = 2,4,6-$Me_3C_6H_2$; 2,6-$Cl_2C_6H_3$; 2,6-$F_2C_6H_3$; 3,4-tBu$_2C_6H_3$; 3,4,5-$(MeO)_3C_6H_2$; 4-BrC_6H_4; 4-MeC_6H_4; and 4-$MeOOCC_6H_4$ at the *meso* positions. The synthesized porphodimethenes and porphyrins have been fully characterized, and the X-ray structure analyses of three representative derivatives are presented.

Introduction

Over the past two decades, the preparation of *meso*-substituted porphyrins with rigid anthracene, biphenylene, or naphthalene spacers has attracted much attention, since they provide a useful platform to introduce various functional groups with precise locations and orientations near the porphyrin backbone. These building blocks have widely been used to determine the distance dependence of photoinduced electron-transfer reactions,[1] to prepare and examine cofacial diporphyrins,[2] and to synthesize bridged porphyrins with well-defined separations and varying relative arrangements of the porphyrin rings.[3] In addition, porphyrins with functionalized anthracene or naphthalene groups have been used as precursors for the synthesis of molecular receptors[4] and for the design of dinuclear complexes.[5] In the latter case, a chelating ligand was bound to the rigid aromatic system, which provides an additional coordination site in a predetermined geometry.

The incorporation of a symmetrically or asymmetrically functionalized linker into the porphyrin backbone is among the most important steps in these synthetic approaches. In general, multistep procedures are required, and in order to vary the type or position of the functional group at the aromatic spacer, new synthetic strategies must be developed. So far, no general concept has been devised to allow for the facile synthesis of porphyrins bearing rigid aromatic spacers with diverse functional groups. The ability to anchor various groups on these rigid spacers offers many exciting opportunities for engineering porphyrin platforms.

Because of the proximity of the functional groups to the macrocyclic ring, porphyrins joined at the 1-position of an 8-substituted naphthalene spacer can be regarded as superior precursors for the design of artificial molecular receptors, sophisticated oxidation catalysts, or models for biological porphyrin-based enzymes. While porphyrins containing a single 8-functionalized naphthalene have been prepared and utilized for diverse purposes including molecular recognition and examination of electronic porphyrin−quinone interactions,[6] we have recently demonstrated the utility of *trans*-α,α- and α,*β*-

* Corresponding author fax: 352-392-3255.

(1) (a) Staab, H. A.; Kratzer, B.; Quazzotti, S. *Eur. J. Org. Chem.* **1998**, *2149*, 9. (b) Staab, H. A.; Hauck, R.; Popp, B. *Eur. J. Org. Chem.* **1998**, *631*, 1. (c) Staab, H. A.; Feurer, A.; Krieger, C.; Kumar, A. S. *Liebigs Ann. Chem.* **1997**, 2321. (d) Staab, H. A.; Feurer, A.; Hauck, R. *Angew. Chem., Int. Ed. Engl.* **1994**, *33*, 2428.

(2) For example: (a) Ward, B.; Wang, C.-B.; Chang, C. K. *J. Am. Chem. Soc.* **1981**, *103*, 5236. (b) Chang, C. K.; Abdalmuhdi, I. *J. Org. Chem.* **1983**, *48*, 5388. (c) Collman, J. P.; Bencosme, C. S.; Durand, R. R.; Kreh, R. P.; Anson, F. C. *J. Am. Chem. Soc.* **1983**, *105*, 2699. (d) Chang, C. K.; Abdalmuhdi, I. *Angew. Chem., Int. Ed. Engl.* **1984**, *23*, 164. (e) Chang, C. K.; Liu, H. Y.; Abdalmuhdi, I. *J. Am. Chem. Soc.* **1984**, *106*, 2725. (f) Eaton, S. S.; Eaton, G. R.; Chang, C. K. *J. Am. Chem. Soc.* **1985**, *107*, 3177. (g) Liu. H.-Y.; Abdalmuhdi, I.; Chang, C. K.; Anson, F. C. *J. Phys. Chem.* **1985**, *89*, 665. (h) Fillers, J. P.; Ravichandran, K. G.; Abdalmuhdi, I.; Tulinsky, A.; Chang, C. K. *J. Am. Chem. Soc.* **1986**, *108*, 417. (i) Collman, J. P.; Kim, K.; Leidner, C. R. *Inorg. Chem.* **1987**, *26*, 1152. (j) Collman, J. P.; Hendricks, N. H.; Kim, K.; Bencosme, C. S. *J. Chem. Soc., Chem. Commun.* **1987**, 1537. (k) Ni, C.-L.; Abdalmuhdi, I.; Chang, C. K.; Anson, F. C. *J. Phys. Chem.* **1987**, *91*, 1158. (l) Collman, J. P. Hutchison, J. E.; Wagenknecht, P. S.; Lewis, N. S.; Lopez, M. A.; Guilard, R. *J. Am. Chem. Soc.* **1990**, *112*, 8206. (m) Naruta, Y.; Maruyama, K. *J. Am. Chem. Soc.* **1991**, *113*, 3595. (n) Collman, J. P.; Hutchison, J. E.; Lopez, M. A.; Tabard, A.; Guilard, R.; Seok, W. K.; Ibers, J. A.; L'Her, M. *J. Am. Chem. Soc.* **1992**, *114*, 9869. (o) Guilard, R.; Lopez, M. A.; Tabard, A.; Richard, P.; Lecomte, C.; Brandes, S.; Hutchison, J. E.; Collman, J. P. *J. Am. Chem. Soc.* **1992**, *114*, 9877 and references therein.

(3) (a) Osuka, A.; Maruyama, K. *J. Am. Chem. Soc.* **1988**, *110*, 4454. (b) Naruta, Y.; Sasayama, M.; Ichihara, K. *Russ. J. Org. Chem.* **1996**, *32*, 214. (c) Cammidge, A. N.; Öztürk, O. *Tetrahedron Lett.* **2001**, *42*, 355.

(4) Liang, Y.; Chang, C. K. *Tetrahedron Lett.* **1995**, *36*, 3817.

(5) (a) Chang, C. K.; Kondylis, M. P. *J. Chem. Soc., Chem. Commun.* **1986**, 316. (b) Bag, N.; Chern, S.-S.; Peng, S. M.; Chang. C. K. *Inorg. Chem.* **1995**, *34*, 753.

(6) Iovine, P. M.; Kellett, M. A.; Redmore, N. P.; Therien, M. J. *J. Am. Chem. Soc.* **2000**, *122*, 8717.

10.1021/jo010163l CCC: $20.00
Published on Web 07/07/2001

8-carboxynaphthylporphyrins bearing two 8-functionalized naphthyl moieties.[8,11,17] These simple molecules have the potential to be useful building blocks for numerous applications, including the preparation of heteronuclear porphyrin arrays and the development of redox-switchable tetrapyrrolic macrocycles.

Given the lack of any suitable procedure, we developed a general two-step synthesis for the preparation of the desired porphyrins, and in addition to allowing for the incorporation of a range of groups on the naphthalene spacer, the steric and the electronic attributes of the aromatic substituents at the *meso* position of the macrocycle can be readily adjusted utilizing this simple methodology. In sharp contrast to traditional pathways for the preparation of porphyrins, we initially prepared and isolated the *spiro* tricyclic-type porphodimethenes by acid-catalyzed condensation of commercially available acenaphthenequinone and readily available 5-aryldipyrromethanes. Ring opening and subsequent porphyrin formation can be induced by either strong bases (KOH, NaOMe), $NaBH_4$, or acids (H_2SO_4, TFA). Herein, we report the details of this synthetic strategy for the preparation of novel building blocks and discuss the structural and the spectroscopic properties of both the porphodimethene precursors and the corresponding porphyrins.

Results and Discussion

Following the [2 + 2] procedures introduced by Lindsey et al.,[7] attempts to react 1,8-naphthalaldehydic acid with 5-aryldipyrromethanes failed to yield the corresponding porphyrins (Scheme 1). The inactivity of this naphthalene derivative toward acid-catalyzed porphyrin formation could possibly be attributed to the strong polar interactions of the adjacent acid function, resulting in a reduced electrophilicity of the aldehyde group, although this issue has not been fully explored with other 1-naphthaldehydes. Even though formation of the tetrapyrrolic porphyrin precursors might be achieved under other conditions, the required oxidation of the porphyrinogens initially formed in the reaction with oxidants such as DDQ will likely cause degradation of the macrocycle.[8]

Scheme 1. Attempted Formation of Porphyrins by Reaction of 5-Mesityldipyrromethane with 1,8-Naphthaldehydic Acid

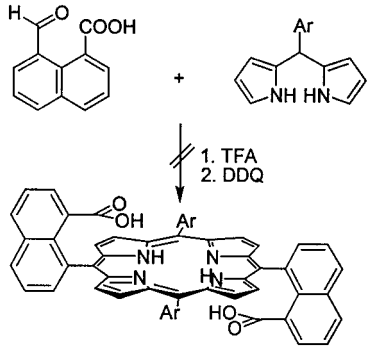

Scheme 2. Preparation of the 5-Acenaphthenone-Substituted Dipyrromethane 1 and Its Ring Opening

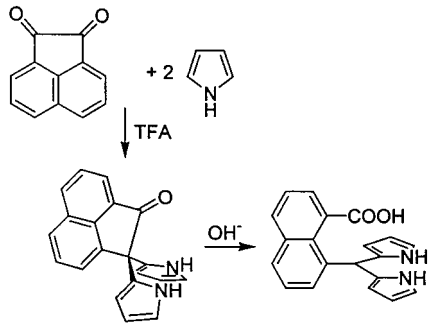

As demonstrated by Chang and co-workers, acenaphthenequinone will condense with 2 equiv of 2-(ethyloxycarbonyl)-3-ethyl-4-methylpyrrole to yield the corresponding dipyrromethane, and refluxing the product in 30% KOH induces the opening of the acenaphthene ring.[5a] Following this approach, we reacted acenaphthenequinone with an excess of pyrrole and isolated the β-unsubstituted dipyrromethane bearing a 1-acenaphthenone moiety at the 5-position (Scheme 2). With this precursor, we reasoned a [2 + 2] condensation with excess aldehyde might yield a mixture of porphodimethenes (*syn* and *anti*) that could then be converted to the desired porphyrins following ring opening and oxidation. In comparison to the acenaphthenone dipyrromethane (**1**), the predilection to form the aromatic porphyrin macrocycle should facilitate the ring-opening reaction for the porphodimethenes. Unfortunately, attempts to react the acenaphthenone-substituted dipyrromethane with various aromatic aldehydes resulted in the formation of complicated mixtures of products, and the desired porphodimethenes were only obtained as minor products. To overcome this difficulty, the dipyrromethane (**1**) precursor was refluxed in 1-propanol in the presence of 30% aqueous KOH to initiate ring opening (Scheme 2), and the free acid (**1a**) was produced after protonation with HCl(aq). The product

(7) (a) Lindsey, J. S.; Hsu, H. C.; Schreiman, I. C. *Tetrahedron Lett.* **1986**, *27*, 4969. (b) Lindsey, J. S.; Schreiman, I. C.; Hsu, H. C.; Kearney, P. C.; Marguerettaz, A. M. *J. Org. Chem.* **1987**, *52*, 827. (c) Lindsey, J. S.; Wagner, R. W. *J. Org. Chem.* **1989**, *54*, 828.

(8) Harmjanz, M.; Gill, H. S.; Scott, M. J. *J. Am. Chem. Soc.* **2000**, *122*, 10476.

(9) (a) Buchler, J. W.; Puppe, L. *Liebigs Ann. Chem.* **1970**, *740*, 142. (b) Dwyer, P. N.; Buchler, J. W.; Scheidt, W. R. *J. Am. Chem. Soc.* **1974**, *96*, 2789. (c) Buchler, J. W.; Puppe, L. *Liebigs Ann. Chem.* **1974**, 1046. (d) Dwyer, P. N.; Puppe, L.; Buchler, J. W.; Scheidt, W. R. *Inorg. Chem.* **1975**, *14*, 1782. (e) Buchler, J. W.; Lay, K.-L. *Z. Naturforsch., B: Chem. Sci.* **1975**, *30*, 385. (f) Buchler, J. W.; Lamlay, K.; Smith, P. D.; Scheidt, W. R.; Rupprecht, G. A.; Kenny, J. E. *J. Organomet. Chem.* **1976**, *110*, 109. (g) Buchler, J. W.; Dreher, C.; Lay, K.-L.; Lee, Y. J. A.; Scheidt, W. R. *Inorg. Chem.* **1983**, *22*, 888. (h) Botulinski, A.; Buchler, J. W.; Lay, K.-L.; Stoppa, H. *Liebigs Ann. Chem.* **1984**, 1259. (i) Botulinski, A.; Buchler, J. W.; Tonn, B.; Wicholas, M. *Inorg. Chem.* **1985**, *24*, 3239. (j) Botulinski, A.; Buchler, J. W.; Abbes, N. E.; Scheidt, W. R. *Liebigs Ann. Chem.* **1987**, 305. (k) Botulinski, A.; Buchler, J. W.; Wicholas, M. *Inorg. Chem.* **1987**, *26*, 1540. (l) Botulinski, A.; Buchler, J. W.; Lee, Y. J.; Scheidt, W. R.; Wicholas, M. *Inorg. Chem.* **1988**, *27*, 927. (m) Renner, M. W.; Buchler, J. W. *J. Phys. Chem.* **1995**, *99*, 8045.

(10) Senge, M. O.; Runge, S.; Speck, M.; Ruhlandt-Senge, K. *Tetrahedron* **2000**, *56*, 8927.

(11) Harmjanz, M.; Scott, M. J. *Chem. Commun.* **2000**, 397.

(12) Král, V.; Sessler, J. L.; Zimmerman, R. S.; Seidel, D.; Lynch, V.; Andrioletti, B. *Angew. Chem., Int. Ed.* **2000**, *39*, 1055.

(13) Bonomo, L.; Solari, E.; Scopelliti, R.; Floriani, C.; Re, N. *J. Am. Chem. Soc.* **2000**, *122*, 5312.

(14) Littler, B. J.; Ciringh, Y.; Lindsey, J. S. *J. Org. Chem.* **1999**, *64*, 2864.

(15) Providing further evidence for this flexing, the ^{1}H NMR spectrum exhibits only two sets of resonances for the pyrrolic protons, and if the macrocycle were to adopt a single conformation, four pairs of protons should be inequivalent.

(16) The *syn* isomers of the porphodimethenes can adopt either an open or closed confirmation with respect to the carbonyl groups, and while **4** displays the closed orientation, the open conformer has been detected in the solid-state structure of a metalated (Zn) *syn* lactonized porphodimethene. See ref 8.

(17) Harmjanz, M.; Scott, M. J. *Inorg. Chem.* **2000**, *39*, 5428.

Table 1. Isolated Yields and Selected Analytical Data for Porphodimethenes 2−17

Aldehyde used	Yield (%)	UV-Vis, λ_{max}(log ε)	^{1}H-NMR (N-H, pyrrolic C-H)
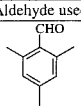	(**2**) *Syn*: 11	440 (4.97)	14.00 (s); 5.94 (d), 6.17 (d)
	(**3**) *Anti*: 15	438 (4.93)	13.92 (s); 6.11 (d), 6.21 (d)
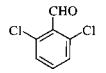	(**4**) *Syn*: 11	440 (4.82)	13.83 (s); 5.96 (d), 6.13 (d)
	(**5**) *Anti*: 12	442 (4.86)	13.79 (s); 6.16 (d), 6.21 (d)
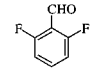	(**6**) *Syn*: 2	441 (4.97)	13.87 (s); 5.98 (d), 6.28 (d)
	(**7**) *Anti*: 5	439 (4.90)	13.83 (s); 6.17 (d), 6.32 (d)
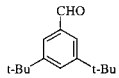	(**8**) *Syn*: 8	442 (4.92)	14.02 (s); 6.02 (d), 6.37 (d)
	(**9**) *Anti*:12	440 (4.82)	14.03 (s); 6.22 (d), 6.43 (d)
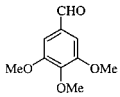	(**10**) *Syn*: 9	446 (4.90)	13.89 (s); 6.00 (d), 6.42 (d)
	(**11**) *Anti*: 15	443 (4.97)	13.91 (s); 6.21 (d), 6.48 (d)
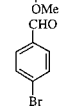	(**12**) *Syn*: 8	442 (4.93)	13.89 (s); 6.00 (d), 6.28 (d)
	(**13**) *Anti*: 6	441 (4.88)	13.89 (s); 6.21 (d), 6.35 (d)
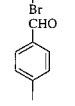	(**14**) *Syn*: 3	442 (4.92)	13.94 (s); 5.98 (d); 6.33 (d)
	(**15**) *Anti*: 12	440 (4.83)	13.94 (s); 6.19 (d); 6.40 (d)
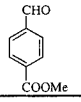	(**16**) *Syn*: 4	442 (4.95)	13.89 (s); 5.98 (d), 6.23 (d)
	(**17**) *Anti*: 4	440 (4.84)	13.91 (s); 6.21 (d), 6.31 (d)

was only slightly soluble in solvents such as methylene chloride or chloroform, and in order to utilize the molecule for the preparation of porphyrins, the carboxylic acid group must be masked to enhance the solubility of the dipyrromethane in the condensation reaction mixture. In view of the increasing number of synthetic steps necessary to produce porphyrins from **1**, efforts to further develop methodologies with these precursors were not undertaken.

With the desire to simplify the procedure, the formation of porphodimethenes was attempted by treating 5-substituted, β-unsubstituted dipyrromethanes (Table 1) with acenaphthenequinone in the presence of catalytic amounts of either $BF_3 \cdot OEt_2$ or TFA (Scheme 3), and as outlined in Table 1, the reaction proved to be quite convenient and versatile. Through simple substitutions of the aryl groups in the dipyrromethane precursors, this general pathway allows for the isolation of the porphodimethenes with different steric and electronic properties. Buchler et al. have extensively studied porphodimethenes, but the preparation of the macrocycle is normally achieved by way of the reductive alkylation of porphyrins,[9] prohibiting the synthesis of aryl-substituted porphodimethenes by this method. Quite recently, several new procedures for the preparation of porphodimethenes have been reported, including the condensation of pyrrole with sterically encumbered aldehydes[10] and the reaction of acetone[11] or vicinal diketones[12] with 5-aryldipyrromethanes. In addition, porphodimethenes can be prepared in convenient quantities by the dealkylation of porphyrinogens,[13] but once again, this methodology cannot be applied to *meso*-aryl-substituted macrocycles.

In the [2 + 2] condensation reactions outlined in Scheme 3, the overall yields of both isomers (*syn* and *anti*) range from 7 (**6** and **7**) to 26% (**2** and **3**), and as witnessed by Lindsey et al. for the formation of porphyrins by [2 + 2] condensations, the yields[7] and the molar ratios of the atropisomers are strongly dependent on the electronic and steric nature of the dipyrromethane starting materials as well as the reaction conditions (nature of the acid, dilution factors, and solvents). Although no concerted attempt was made to maximize the yields for the respective porphodimethenes by varying conditions, the procedures optimized for the preparation of porphyrins have been utilized throughout.[14] For the first step in the purification process, the reaction mixtures were filtered through a column of neutral alumina, allowing for the quick isolation of a mixture of the porphodimethenes, *syn* and *anti*. The two isomers can then be separated by column chromatography (silica gel) with ether (**10**, **11**,

Scheme 3. General Two-Step Synthetic Pathway for the Preparation of Porphyrins[a]

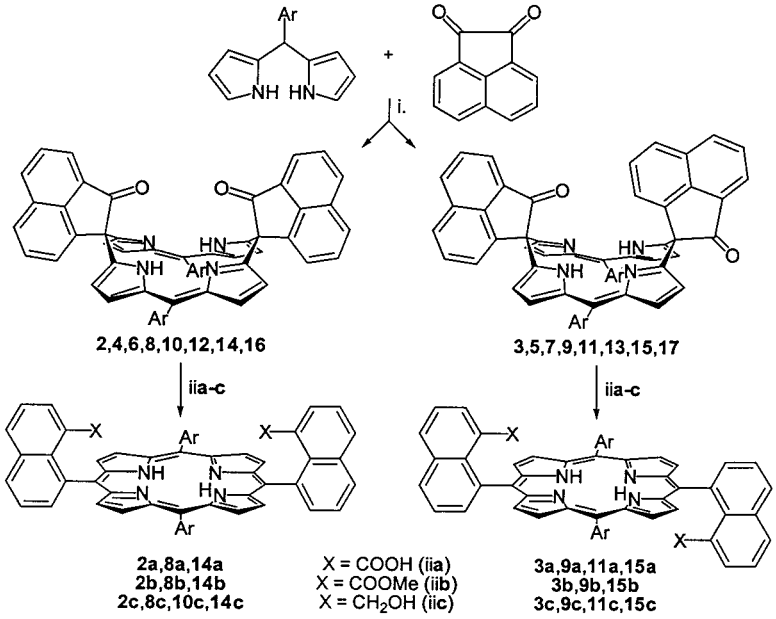

[a] Reagents and conditions: (i) 1, TFA or $BF_3 \cdot OEt_2$, CH_2Cl_2; 2, DDQ. (iia) 30% KOH(aq), reflux (THF), air. (iib) 1, NaOMe (THF/MeOH) rt; 2, O_2. (iic) $NaBH_4$ (THF/MeOH), rt, air.

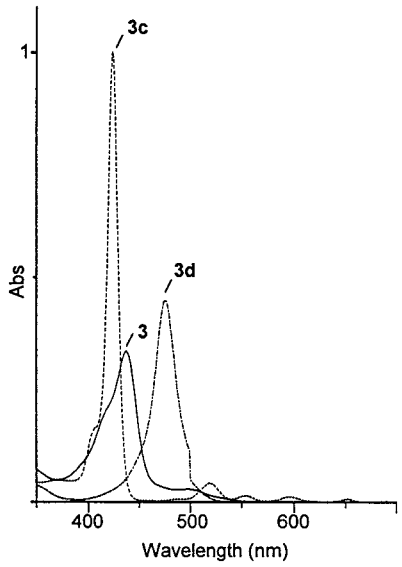

Figure 1. UV−vis spectra of the porphodimethene **3** (Ar = mesityl), the Zn(II) complex **3d**, and the porphyrin−dialcohol **3c** within the region of 350−700 nm.

16, and **17**), toluene (**2**, **3**, **8**, **9**, **14**, and **15**), or a CH_2Cl_2/hexanes mixture as the eluting solvent (**4**−**7**, **12**, and **13**); the *anti* derivatives are isolated first.

The respective porphodimethene isomers (*syn* and *anti*) are both bright orange solids and exhibit a characteristic absorption maxima in the UV−vis spectra ranging from 438 (**3**) to 446 nm (**10**) (Figure 1). In comparison to *meso*-alkylporphodimethenes (417−426 nm),[9g,12] the main absorption bands are batochromically shifted but exhibit similar logarithmic extinction (log ϵ) coefficients ranging from 4.82 (**4**, **9**) to 4.97 (**2**, **11**) (Table 1).

Despite the diverse nature of aryl substituents that have been introduced into the porphodimethene, no significant correlation was observed between the electronic and steric properties of the aryl moiety and the dipyrromethene band in the UV−vis spectra. The two isomers can easily be distinguished by ^{1}H NMR spectroscopy, and the resonances associated with the pyrrolic protons are compiled in Table 1. All of the porphodimethenes exhibit two sets of doublets for the pyrrolic C−H protons, typically between 6.0 and 6.5 ppm, in sharp contrast to the analogous signals for porphyrins normally found above 8 ppm. This behavior may be attributed to the disruption of electron delocalization within the macrocycle, increasing the shielding of the pyrrolic protons. Further highlighting the lack of aromaticity of the porphodimethenes, the resonances for the N−H protons appear far downfield shifted [13.79 (**5**)−14.03 (**9**) ppm] in the ^{1}H NMR spectra. Interestingly, the spectra of the *anti* isomers consistently display only one set of signals for the naphthalene and the *meso*-aryl substituents, even though the rooflike folded structure with its *spiro*-locked acenaphthenenones would implicate two sets of signals. For instance, the *o*-methyl and the aromatic (mesityl) protons of the *anti*-mesityl derivative **3** each exhibit a single resonance in the ^{1}H NMR spectrum. Moreover, in the aromatic region, the typical two double doublets and four doublets from two indistinguishable acenaphthenone moieties are observed. While free rotation about the $C_{meso}-C_{aryl}$ bond could arguably give rise to singlets for the mesityl substituents, the presence of a single set of

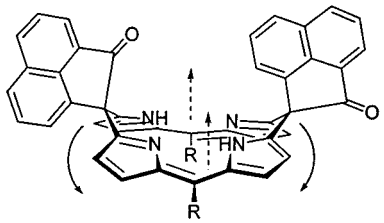

Figure 2. Conformational flexing of the porphodimethene macrocycle.

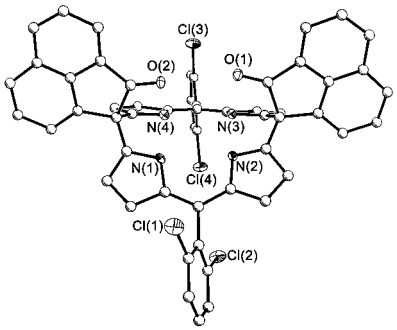

Figure 3. ORTEP diagram of the solid-state structure of **4** (30% probability, carbons arbitrary radii). H-atoms omitted for clarity.

signals for the acenaphthenones insinuate a different mechanism, and on the basis of these observations, it appears that the porphodimethenes undergo a fast flexing of the two dipyrromethane units along a line joining the two saturated meso carbons (Figure 2) in solution. The low temperature ^{1}H NMR spectrum of the *anti*-3,5-tBu$_2$C$_6$H$_3$ derivative **12** reveals significant broadening of some of the signals for the naphthalene protons as well as the signals from the pyrrolic and aromatic [3,5-tBu$_2$C$_6$H$_3$] protons. Even at −80 °C, no splitting of these broadened peaks could be detected, suggesting a fast equilibrium between these two possible conformers.[15] Further highlighting the flexibility of the porphodimethene framework, metalation with zinc (**3d**) induces significant flattening of the macrocycle relative to the free porphodimethene **3**.[11] In addition, two conformers can be envisioned for the *syn* isomer, each adopting the rooflike folded structure typical for porphodimethenes.

Figure 3 displays the solid-state structure of the 2,6-dichlorophenyl-substituted *syn*-porphodimethene (**4**). The two saturated carbon atoms force the tetrapyrrolic macrocycle to adopt a strong rooflike folded structure with an interplanar roof angle of 123.1°, whereby the two carbonyl oxygens are pointing toward each other (O···O distance: 2.95 Å). The macrocycle adopts this conformational arrangement (*cis*) as it corresponds to the energetically preferred binding situation of this tricyclic *dispiro* conformer in the solid state.[16] As expected, the two dihedral angles at the meso carbons, defined by the five-membered ring of the acenaphthenone and the adjacent pyrrole carbons, respectively, deviate only slightly from 90° (90.3 and 88.9°).

Metalation of the Porphodimethenes. The ability to metalate the porphodimethenes prior to the ring-opening reactions is an important issue in the design of novel porphyrin-based ligand systems or cofacial single-stranded porphyrin arrays.[17] In particular, the development of heterometallic systems, which involves different metal ions in the chromophoric backbone and the at-

Table 2. Isolated Yields and λ_{max} for Metalated [Zn(II), Cu(II), and Co(II)] Porphodimethenes

Aryl substituent	Metal ion	Yield (%)	UV-Vis, λ_{max}(log ε)
	Zn(II)	(**2d**) *Syn*: 97	477 (5.13)
		(**3d**) *Anti*: 91	475 (5.17)
	Cu(II)	(**2e**) *Syn*: 99	486 (5.08)
		(**3e**) *Anti*: 98	483 (5.09)
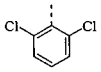	Zn(II)	(**4d**) *Syn*: 95	484 (5.10)
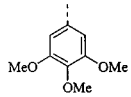	Cu(II)	(**11e**) *Anti*: 95	483 (5.08)
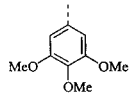	Co(II)	(**11f**) *Anti*: 94	482 (4.51)

tached peripheral ligand system, may be envisioned by metalation of the porphodimethene followed by the generation of the functionalized porphyrin and the introduction of the second metal ion.[17] Although the porphodimethenes (**2**−**17**) enclose carbonyl groups as weak peripheral donor functions, only minor coordinative interactions with metal ions are to be expected due to their distance and orientation relative to the four nitrogen donors. Consequently, the deprotonated porphodimethenes can, in principle, be viewed as tetradentate macrocycles with two negative charges. As an initial entry into the chemistry of these macrocycles, the neutral Cu(II) and Zn(II) complexes of the porphodimethenes **2** and **3** (Ar = mesityl) and the Co(II) complex of the *anti* derivative **11** [Ar = 3,4,5-$(MeO)_3C_6H_2$] were prepared. Metalation was achieved in high yields by refluxing the porphodimethenes in a chloroform−methanol mixture in the presence of the respective metal salts [$Zn(OAc)_2 \cdot 2H_2O$ (**2d**, **3d**, and **4d**), $Cu(OAc)_2 \cdot H_2O$ (**2e**, **3e**, and **11e**), and $Co(OAc)_2 \cdot 4H_2O$ (**11f**)] (Table 2). Because the main absorption band of the porphodimethenes experiences a significant bathochromic shift after metalation, the reaction progress can easily be monitored by UV−vis spectroscopy (Figure 1). Compared to the metal-free porphodimethenes [log ϵ = 4.97 (**2**) and 4.93 (**3**)], a strong increase [log ϵ = 5.13 (**2d**), 5.08 (**2e**), 5.17, (**3d**), and 5.09 (**3e**)] of the extinction coefficient is observed after incorporation of Zn(II) or Cu(II) into the chromophoric ligand. In contrast, complexation of Co(II) by the porphodimethene (**11**) induces a considerable decrease of the extinction coefficient. As a general trend, the separation between the two doublets arising from the pyrrolic protons in the ^{1}H NMR spectra of the three diamagnetic Zn complexes (**2d**−**4d**) increases in comparison to the metal-free porphodimethenes [0.27 (**2d** and **4d**)−0.44 (**3d**) vs 0.1 (**3**)−0.23 (**2**)]. These changes might be traced back to both the altered electronic situation within the dipyrromethene halves and the modified structural configuration of the macrocycle after metalation.

The solid-state structure of the *syn*-zinc-mesityl porphodimethene **4d** is outlined in Figure 4.[18] Relative to the unmetalated porphodimethene **4** (123.1°), the interplanar angle defined by the dipyrromethene units is slightly more obtuse (131.3°). With the two carbonyl groups situated close to each other above the plane of the macrocycle, the "closed" arrangement of the porphodimethene does not allow for an interaction of the Zn center with external ligands, as observed for the related *anti*-zinc-mesityl porphodimethene **3d**.[11] Lacking the ability to bind to an additional ligand, the Zn is coordinated by the four pyrrolic nitrogens and interacts with one of the adjacent carbonyl oxygen atoms [Zn−O: 2.311-(7) Å]. As a consequence of this highly distorted square pyramidal coordination environment, the Zn−N distances vary from 2.037(8) to 2.071(8) Å, and the metal resides 0.443 Å above the plane defined by these four pyrrole donor atoms [0.404 Å (**3**)].[11]

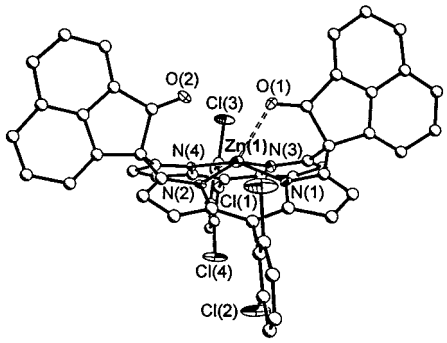

Figure 4. ORTEP diagram of the solid-state structure of **4d** (30% probability, carbons arbitrary radii). H-atoms omitted for clarity. Selected distances (Å) and angles (deg): Zn(1)−N(1), 2.071(8); Zn(1)−N(2), 2.069(8); Zn(1)−N(3), 2.037(8); Zn-(1)−N(4), 2.059(8); Zn(1)−O(1), 2.311(7); N(1)−Zn(1)−N(2), 86.5(3); N(2)−Zn(1)−N(3), 87.9(3); N(3)−Zn(1)−N(4), 86.6(3); N(1)−Zn(1)−N(4), 88.4(3).

Formation of Porphyrins. (a) Ring-Opening Reactions with KOH and NaOMe. To generate the aromatic porphyrin macrocycle, a carbon−carbon bond in each of the *spiro*-linked acenaphthenone moieties must be broken, and as found in our initial studies, refluxing the respective porphodimethenes (*syn* and *anti*) in THF in the presence of 30% KOH will induce the opening of this ring. Presumably, the nucleophilic attack of the hydroxide anion at the carbonyl carbon initiates the ring-opening reaction, and the resulting species is subject to oxidation in the presence of dioxygen, rapidly forming the porphyrin macrocycle. Subsequent protonation with HCl(aq) yields the corresponding free diacids of the *trans*-8-carboxynaphthyl-functionalized porphyrins; in the absence of acid, the dipotassium salts can be isolated. Despite these rather harsh reaction conditions, no interconversion between α,α- and α,*β*-isomers has thus far been detected. The isolation and purification of the α,*β*-free acids have been severely hampered by the insolubility of these materials in common organic solvents. Fortunately, these materials can be isolated directly by precipitation from the reaction mixture as the dipostassium salts, and they can be further purified by recrystallization from methanol/ether solutions. In sharp contrast, the α,α-isomers are highly soluble. The insolubility of the α,*β*-free acids may be attributed to intermolecular hydrogen bonding interactions between the acid groups, which are aligned above and below the porphyrin plane. On the basis of the rigidly predefined positions of the functional groups, these compounds have the strong

(18) Two independent molecules of **4d** occur in the asymmetric unit. Data given and discussed within the text are only for one molecule. For details, see the Supporting Information.

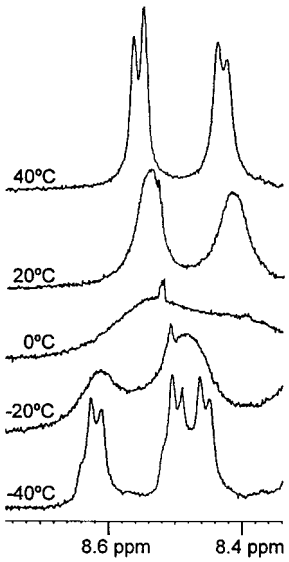

Figure 5. Temperature-dependent NMR spectra of the pyrrole protons in **3a**.

tendency to form infinite single-stranded porphyrin arrays, as illustrated by the X-ray structure analysis of the dipotassium salt **3a** and by the preparation of several heterometallic cofacial porphyrin arrays.[17] As indicated by the ^{1}H NMR spectra of the free-base porphyrin dipotassium salts, the trend toward the formation of higher aggregates appears to be observable in solution. While the two peaks for the two chemically distinct pyrrole protons are significantly broadened at rt, the splitting of these resonances into two doublets (J = 4.4 Hz), typical of 2 + 2 porphyrins, is only evident at higher temperatures (40 °C) (Figure 5). This behavior could be explained by a back and forward movement of the naphthalene moiety toward the plane normal to the porphyrin backbone. At lower temperatures (0 °C), the doublets merge together, and at −40 °C, a splitting into three doublets can be observed. As previously witnessed in the solid-state structure of the dipotassium salt, the angles between the naphthalene planes and the porphyrin ring deviate significantly from 90° (74.8°). Consequently, the formation of higher aggregates in low-temperature solutions can impose comparable naphthalene to porphyrin angles, inducing the chemical shifts for the four pyrrolic protons to be inequivalent. Alternatively, these findings may also be rationalized by a temperature-dependent potassium ion migration between the carboxylates and the pyrrolic nitrogens.

Reactions with KOH have also been undertaken with metalated [Zn(II) and Cu(II)] porphodimethenes to yield the corresponding metalated porphyrin species. The overall yields for the ring-opening reaction are highly dependent on both the properties of the *meso*-aryl substituents bound at the porphyrin and the nature of the metal ions incorporated into the macrocycle (Table 3). Yields between 45% for the copper derivative **11h** (Ar = 3,4,5-$(MeO)_3C_6H_2$) and 92% for the free-base porphyrin **2a** (Ar = mesityl) have been found. In general, higher yields are obtained for the unmetalated derivatives, since the metalated compounds are more prone to undergo ring closure by oxidative lactonization and formation of *dispiro*, tricyclic, *meso*-C/O bound porphodimethenes.[8]

Inasmuch as the main absorption bands (Soret band) of the porphyrins appear at markedly lower wavelengths

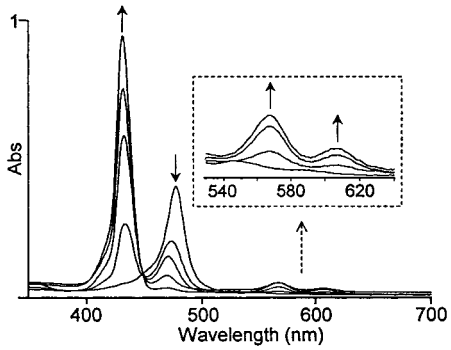

Figure 6. UV−vis spectra of **2** upon reaction with 30% KOH in boiling THF, forming **2d**. The arrows indicate the direction of change in the peaks during porphyrin formation.

Table 3. Isolated Yields and λ_{max} for the Porphyrin Products Depicted in Scheme 1

aryl substituent	M	X, method	atropisomer	yield (%)	UV−vis (λ_{max})
2,4,6-$Me_3C_6H_2$		COOH, KOH	α,α: **2a**	92	432
2,4,6-$Me_3C_6H_2$	Zn	COOH, KOH	α,α: **2g**	75	431
2,4,6-$Me_3C_6H_2$		COOK, KOH	α,β: **3a**	65	431
2,4,6-$Me_3C_6H_2$	Zn	COOK, KOH	α,β: **3g**	46	430
2,4,6-$Me_3C_6H_2$	Cu	COOK, KOH	α,β: **3h**	65	421
3,5-(t-Bu)$_2C_6H_3$		COOH, KOH	α,α: **8a**	78	426
3,5-(t-Bu)$_2C_6H_3$		COOK, KOH	α,β: **9a**	90	427
3,4,5-$(OMe)_3C_6H_2$	Cu	COOK, KOH	α,β: **11h**	45	422
4-MeC_6H_4		COOH, KOH	α,α: **14a**	83	426
4-MeC_6H_4		COOK, KOH	α,β: **15a**	77	432
2,4,6-$Me_3C_6H_2$		COOMe, NaOMe	α,α: **2b**	69	425
2,4,6-$Me_3C_6H_2$		COOMe, NaOMe	α,β: **3b**	81	425
3,5-(t-Bu)$_2C_6H_3$		COOMe, NaOMe	α,α: **8b**	71	426
3,5-(t-Bu)$_2C_6H_3$		COOMe, NaOMe	α,β: **9b**	60	426
4-MeC_6H_4		COOMe, NaOMe	α,α: **14b**	68	426
4-MeC_6H_4		COOMe, NaOMe	α,β: **15b**	60	426
2,4,6-$Me_3C_6H_2$		CH_2OH, $NaBH_4$	α,α: **2c**	98	424
2,4,6-$Me_3C_6H_2$		CH_2OH, $NaBH_4$	α,β: **3c**	98	424
3,5-(t-Bu)$_2C_6H_3$		CH_2OH, $NaBH_4$	α,α: **8c**	95	426
3,5-(t-Bu)$_2C_6H_3$		CH_2OH, $NaBH_4$	α,β: **9c**	98	424
3,4,5-$(OMe)_3C_6H_2$		CH_2OH, $NaBH_4$	α,α: **10c**	97	427
3,4,5-$(OMe)_3C_6H_2$		CH_2OH, $NaBH_4$	α,β: **11c**	97	424
4-MeC_6H_4		CH_2OH, $NaBH_4$	α,α: **14c**	95	424
4-MeC_6H_4		CH_2OH, $NaBH_4$	α,β: **15c**	97	424

with considerably higher intensity as compared to the metalated porphodimethenes, the progress of the porphyrin formation reaction with these compounds can be easily monitored by UV−vis spectroscopy. Figure 6 depicts the UV−vis spectra of the *syn*-porphodimethene **2** (Ar = mesityl and M = Zn) upon reaction with KOH in refluxing THF. Besides the aforementioned alteration of the main absorption band, the formation of the characteristic Q-bands within the region between 540 and 640 nm is evident, concomitant with a color change of the reaction mixture from dark orange to dark purple.

Other nucleophiles will react with the porphodimethenes, and the ring-opening can be accomplished with freshly prepared NaOMe in an air- and water-free THF/methanol mixture to yield the corresponding 8-methoxycarbonylnaphthyl functionalized porphyrins. To avoid formation of the favored diacid, water must be rigorously excluded from the reaction mixture, and in contrast to the hydroxide reaction, the transformation readily occurs at rt. To provide an oxidant, dry dioxygen is bubbled through the initially dark green solution prior to the addition of water or an aqueous NH_4Cl solution. The diesters can typically be obtained in yields from 60 (**9b**

and **15b**) to 81% (**3b**) (Table 3) after column chromatography (silica gel, CH_2Cl_2/hexane mixtures as eluants). Utilizing the same reaction conditions, less soluble porphodimethenes such as the 2,6-dichlorophenyl derivative cannot be converted to the desired diesters, since the initially formed porphodimethene disodium salts readily precipitate from the reaction mixture.

(b) Ring-Opening Reaction with $NaBH_4$. Given that porphyrins bearing two hydroxymethyl functions at the 8-position of a naphthalene spacer would be highly desirable building blocks for the preparation of novel organic and inorganic compounds, we attempted to reduce the porphyrin diesters with $LiAlH_4$, but the reaction produced the desired dialcohols in very poor yields. Reduction of the 5-acenaphthenone-substituted dipyrromethane **1** with $NaBH_4$ generates a racemic mixture of the alcohol without ring opening,[21] but in view of the sensitivity of the porphodimethenes to strong bases or acids and the considerable driving force toward porphyrin formation, we reasoned that the ring opening of the porphodimethenes might be achieved with simple reducing agents. Reaction of the porphodimethenes **2**, **3**, **8**−**11**, **14**, and **15** (Table 3) with an excess of $NaBH_4$ in THF/methanol open to air yields the desired porphyrins in almost quantitative yields.

If the reaction is carried out under rigorous air- and water-free conditions, a brilliant green solution forms, which turns dark brown-green after a few minutes. The UV−vis spectrum of the solution (**3** + $NaBH_4$) exhibits an absorption band at 433 nm with a shoulder at 447 nm, and it also displays an unusual broad band at 820 nm. Although this spectrum is not consistent with the UV−vis spectra of two-electron-reduced metalated porphyrin species such as $[TPP-Zn]^{2-}$,[19] the absence of a metal in the macrocycle may allow for the formation of the reduced porphyrin sodium salts. When the green solution is exposed to air, the broad band at 820 nm slowly decreases while the Soret band (425 nm) and the characteristic Q-bands grow in, indicating the formation of the porphyrin (Figure 7). As expected and confirmed by ^{1}H NMR and X-ray structure analyses of **2c**, reactions of the *syn*-porphodimethenes with $NaBH_4$ exclusively produce the α,α-atropisomers, while the analogous reactions of the *anti*-porphodimethenes yield the α,*β*-atropisomers. Although we restricted our investigation to alkyl- and methoxy-substituted *meso*-arylporphyrins, this reaction should be applicable for the preparation of *trans*-8-hydroxymethylnaphthylporphyrins containing other substitution patterns at the *meso*-aryl substituents. Relative to the 8-carboxynaphthylporphyrins, the dialcohols exhibit enhanced stability in air; nevertheless, in the presence of strong oxidants, they also undergo a ring-closing reaction to form porphodimethenes.[8,20]

Figure 8 displays an ORTEP plot of **2c**, and in the solid-state, one of the naphthalene spacers exhibits two distinct inclinations relative to the porphyrin plane, each with a site occupancy factor of 0.5. For clarity, only one position is shown in Figure 8, but for the discussion, mean values of the two positions are given. Compared to the α,*β*-diester **3b** (61.8°),[11] the porphyrin plane (defined by the four nitrogen atoms) and the plane

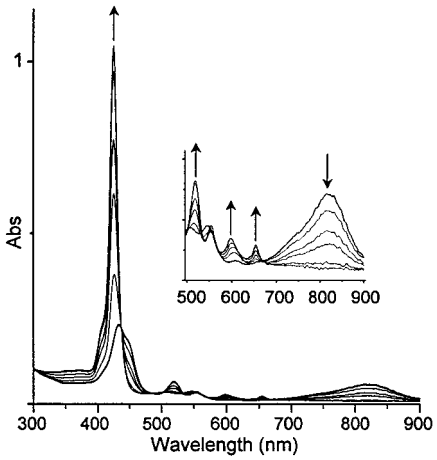

Figure 7. UV−vis spectrum of the green intermediate formed from the reaction of **3** with $NaBH_4$ in THF/MeOH and time course spectra of the reaction mixture after exposure to air. The arrows indicate the direction of change in peaks during porphyrin formation.

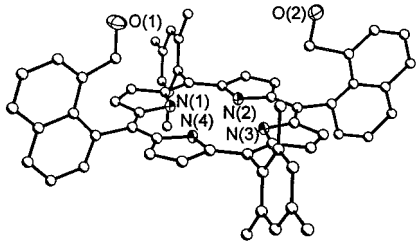

Figure 8. ORTEP diagram of the solid-state structure of **2c** (30% probability, carbons arbitrary radii). H-atoms omitted for clarity. One of the naphthyl groups was disordered across two positions, each with a site occupancy of 0.5, and only one orientation has been depicted.

defined by the naphthalene spacer, respectively, deviate only slightly from 90° (94.0 and 99.5°), and as a result, the two hydroxymethyl carbons are situated 2.85 Å [2.793(8) and 2.913 (8), respectively] above the porphyrin plane with an oxygen−oxygen separation of 7.56 Å. To minimize electronic repulsion between the electron cloud of the porphyrin macrocycle and the alcohol groups, the two hydroxy groups are directed away from the porphyrin plane with the two oxygen−carbon bonds almost parallel to the pseudo-C_2 axis of the molecule.

(c) Ring-Opening Reactions with Acids. Acid-induced ring opening of the *spiro*-linked acenaphthenones also affords the aromatic porphyrin macrocycles. As observed, addition of strong acids such as HCl or H_2SO_4 to a solution of the porphodimethenes will cause ring opening at rt. If the reactions are undertaken in the presence of water, the protonated porphyrin diacid is obtained and the free-base porphyrin is generated after washing the product with water. Prior to ring opening, the N-protonated macrocycle is formed, as demonstrated by UV−vis spectroscopy and an X-ray structure analysis of the protonated porphodimethene **8**.[21] The protonation induces a split in the primary absorption band of **8** (442 nm) into two bands (411 and 478 nm) with lower and higher absorptivity (Figure 9). In the solid-state, the protonated tetrapyrrolic macrocycle severely distorts from planarity, and presumably, the drive to develop aromaticity helps induce the ring-opening reaction and subsequent porphyrin formation.

(19) Closs, G. L.; Closs, L. E. *J. Am. Chem. Soc.* **1963**, *85*, 818.
(20) Confirmed by cyclic voltammetry: Harmjanz, M.; Gill, H. S.; Scott, M. J. Manuscript in preparation.
(21) Harmjanz, M.; Gill, H. S.; Scott, M. J. Unpublished results.

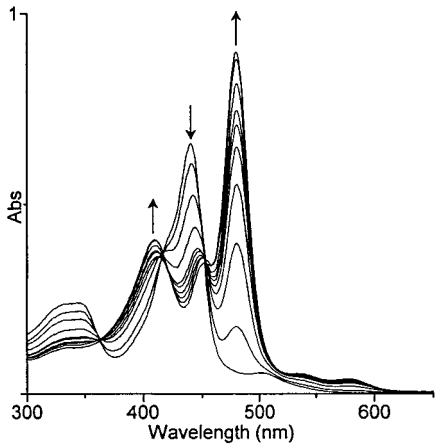

Figure 9. UV−vis spectra of **8** after addition of TFA. The arrows indicate the direction of change in the peaks during protonation.

If methanol is added to the acid-catalyzed reactions with the exclusion of water, the diester porphyrins are obtained in high yields [87 (**8b**), 94 (**9**), and 85% (**15**)]. These reactions must be carried out under a dry O_2 atmosphere with freshly distilled solvents, and concentrated sulfuric acid has been used as the proton source. No interconversion between the *syn* and *anti* derivatives was observed in this reaction. In comparison to the methoxide ring-opening reaction discussed above, the yields for these diesters are higher by the acid-catalyzed route, and this procedure is ideal for the conversion of base-sensitive porphodimethene precursors to porphyrins.

Conclusions

In an effort to prepare a wide range of *trans*-porphyrins incorporating two 8-functionalized naphthalene spacers, a simple, two-step synthetic approach starting from commercially available acenaphthenequinone and readily available 5-aryldipyrromethanes has been developed. This methodology involves the preparation of novel *dispiro* tricyclic porphodimethenes employing a [2 + 2] acid-catalyzed condensation reaction under Lindsey conditions. The porphodimethenes can be metalated [Cu(II), Zn(II), and Co(II)] in high yields, and both the metal-bound and free porphodimethenes can be converted to the corresponding porphyrins. By utilizing KOH, NaOMe, or $NaBH_4$, the respective 8-carboxynaphthyl-, the 8-methoxycarbonylnaphthyl-, and the 8-hydroxymethylnaphthyl-substituted *trans*-porphyrins can be prepared. Alternatively, the porphyrin formation can be achieved at rt with water or methanol in the presence of strong acids. With the diverse nature (acid/base) of the ring-opening reactions and the variety of functionalities that can be incorporated at both the *meso*-aryl moieties and the naphthalene spacer, this work reveals a facile synthetic approach toward the syntheses of sterically and electronically diverse porphyrins with functional groups placed directly above and/or below the macrocycles. The generality of the synthetic pathways will be quite helpful for improving existing efforts to establish porphyrin functionalizations not only in the peripheral surrounding of the macrocyclic plane but also in well-defined axial directions. Efforts to extend the synthetic pathways presented herein to other vicinal diketones as well as the derivatization of the prepared compounds are currently underway.

Experimental Section

The University of Florida Mass Spectrometry Services measured all mass spectral data. Elemental analyses were performed by either Mikroanalytisches Laboratorium H. Kolbe, Mühlheim a. d. Ruhr, Germany or Atlantic Microlabs, Norcross, GA. All 5-aryldipyrromethanes required for the preparation of **2**−**17** have been synthesized according to literature procedures.[22] The dipyrromethane precursors were purified by the following procedure: After removal of the excess pyrrole, the crude product mixtures were filtered through neutral alumina with either CH_2Cl_2 or a CH_2Cl_2/hexanes mixture as the eluant. The solvents were removed in vacuo; the residues were carefully washed with hexanes, pentane, or cyclohexane and dried. This methodology allows for the convenient isolation of the dipyrromethanes in multigram quantities. The products can be further purified by recrystallization.

When $BF_3{\cdot}OEt_2$ was employed for the formation of the porphodimethenes, the reactions were carried out under argon with dried and degassed solvents. The reaction of the porphodimethenes (**2**, **3**, **8**, **9**, **14**, and **15**) with NaOMe for the preparation of the diesters **2b**, **3b**, **8b**, **9b**, **14b**, and **15b** and the acid-catalyzed ring-opening reactions were all performed under Schlenk conditions with dried and degassed solvents. Porphyrin diacids, dialcohols, and dipotassium salts have been found to undergo oxidative ring-closing reactions over time in the presence of air, and these compounds should be stored under an inert atmosphere.

Synthesis of 2,2-Bis-(1*H*-pyrrol-2-yl)-2*H*-acenaphthylen-1-one, 1. A sample of acenaphthenequinone (5 g, 27.4 mmol) was dissolved in 100 mL of freshly distilled pyrrole, and 1 mL of $BF_3{\cdot}OEt_2$ (7.90 mmol) was added. After the reaction mixture was stirred for 45 min, 150 mL of CH_2Cl_2 was added, and the mixture was subsequently treated with 150 mL of 0.1 N NaOH. The organic layer was washed with 150 mL of water (2×) and dried over $NaSO_4$. The solvent and the excess pyrrole were removed in vacuo, and the solid was purified by filtration through neutral alumina (CH_2Cl_2). Yield: 3.7 g (45%). UV−vis (CH_2Cl_2) λ_{max}, nm: 321, 342. ^{1}H NMR (300 MHz, $CDCl_3$): δ 8.55 (bs, 2H), 8.14 (d, 1H, J = 7.9 Hz), 8.00 (d, 1H, J = 6.7 Hz), 7.89 (dd, 1H, $J_1 = J_2$ = 4.5 Hz), 7.69−7.77 (m, 3H), 6.72−6.74 (m, 2H), 6.09 (q, 2H), 5.95−5.97 (m, 2H). HRMS−FAB (*m*/*z*): M^+ calcd for $C_{20}H_{14}N_2O$, 298.1106; found, 298.1105.

Synthesis of 5-(8-Carboxy-1-naphthyl)dipyrromethane, 1a. A sample of the dipyrromethane **1** (500 mg, 1.68 mmol) was dissolved in 15 mL of hot 1-propanol, and 1 mL of 30% KOH(aq) was added. The reaction mixture was refluxed for 45 min, and the solvents were subsequently removed in vacuo. The brown residue was redissolved in THF and acidified with 10 mL (2 N) of HCl. A 15-mL portion of CH_2Cl_2 was added, and the organic phase was separated and subsequently washed with water (3×). After being dried over Na_2SO_4, the solvents were evaporated, and 4 mL of CH_2Cl_2 was added to the residue. After being cooled to 5 °C for 1 h, the microcrystalline, colorless precipitate was filtered off, washed with a small amount of cold CH_2Cl_2, and dried in vacuo to yield 170 mg (32%) of **1a**. ^{1}H NMR (300 MHz, acetone-d_6): δ 9.50 (bs, 2H), 8.05 (dd, 1H, J_1 = 1.4, J_2 = 8.2 Hz), 7.87 (dd, 1H, J_1 = 2.1, J_2 = 7.3 Hz), 7.76 (dd, 1H, J_1 = 1.4, J_2 = 7.04 Hz), 7.44−7.52 (m, 3 H), 6.66 (q, 2H), 6.44 (s, 1H), 5.91 (q, 2H), 5.57−5.59 (m, 2H). HRMS−FAB (*m*/*z*): MH^+ calcd for $C_{20}H_{16}N_2O_2$, 316.1211; found, 316.1216.

General Procedure for the Preparation of the Porphodimethenes (2−17). (a) Synthesis of *syn-dispiro*-[2*H*-Acenaphthylen-1-one-2,5′-10′,20′-dimesityldihydroporphyrin-15′,2″-2″*H*-acenaphthylen-1″-one], 2. *anti*-

(22) (a) Lee, C.-H.; Lindsey, J. S. *Tetrahedron* **1994**, *50*, 11427. (b) Beavington, R.; Burn, P. L. *J. Chem. Soc., Perkin Trans. 1* **1999**, 583.

***dispiro*[2*H*-Acenaphthylen-1-one-2,5′-10′,20′-dimesityldihydroporphyrin-15′,2″-2″*H*-acenaphthylen-1″-one], 3.** A portion of 2.064 g of acenaphthenequinone (11.34 mmol) and 3.000 g (11.34 mmol) of 5-mesityldipyrromethane were dissolved in 1200 mL of CH_2Cl_2, and 0.62 mL (4.9 mmol) of $BF_3 \cdot OEt_2$ was added. After 3 h, 2.580 g of DDQ (11.34 mmol) was added to the greenish-blue solution and the mixture stirred for 1 h. The volume was reduced by 90%, and the mixture was loaded onto an alumina column (CH_2Cl_2, 25 × 4 cm) and slowly eluted with CH_2Cl_2. The solvent of the orange fraction was removed, and the residue was presorbed on silica. The two isomers (**2** and **3**) were separated by silica chromatography (15 × 4 cm, toluene). **2**: Yield: 0.534 g (11%). Anal. Calcd for $C_{60}H_{44}N_4O_2 \cdot 0.25CH_2Cl_2$: C, 82.77; H, 5.13; N, 6.41. Found: C, 83.24; H, 5.29; N, 6.32. UV−vis (CH_2Cl_2) λ_{max}, nm (log ϵ): 440 (4.97). ^{1}H NMR (300 MHz, $CDCl_3$): δ 14.00 (s, 2H, NH), 8.20 (d, 2H, J = 8.1 Hz), 8.15 (d, 2H, J = 7.0 Hz), 8.04 (d, 2H, J = 8.3 Hz), 7.98 (d, 2H, J = 7.0 Hz), 7.85 (dd, 2H, J_1 = 8.2, J_2 = 7.0 Hz), 7.81 (dd, 2H, J_1 = 8.1, J_2 = 7.0 Hz), 6.89 (s, 2H), 6.82 (s, 2H), 6.17 (d, 4H, J = 4.3 Hz), 5.94 (d, 4H, J = 4.3 Hz) 2.31 (s, 6H), 2.23 (s, 6H), 2.19 (s, 6H). HRMS−FAB (*m*/*z*): MH^+ calcd for $C_{60}H_{45}N_4O_2$, 853.3543; found, 853.3569. **3**: The *anti* isomer **3** was collected as the first fraction from the silica column. Yield: 720 mg (15%). Anal. Calcd for $C_{60}H_{44}N_4O_2 \cdot 0.25CHCl_3$: C, 81.97; H, 5.05; N, 6.35. Found: C, 81.99; H, 5.34; N, 6.26. UV−vis (CH_2Cl_2) λ_{max}, nm (log ϵ): 438 (4.93). ^{1}H NMR (300 MHz): δ 13.92 (s, 2H, N−H), 8.76 (dd, 2H, J_1 = 5.4, J_2 = 2.4 Hz), 8.22 (d, 2H, J = 8.1 Hz), 8.17 (d, 2H, J = 7.1 Hz), 8.03 (d, 2H, J = 5.4 Hz), 8.01 (d, 2H, J = 2.4 Hz), 7.82 (dd, 2H, J_1 = 8.1, J_2 = 7.1 Hz), 6.85 (s, 4H), 6.21 (d, 4H, J = 4.2 Hz), 6.11 (d, 4H, J = 4.2 Hz), 2.31 (s, 6H), 2.07 (s, 12H). HRMS−FAB (*m*/*z*): MH^+ calcd for $C_{60}H_{45}N_4O_2$, 853.3543; found, 853.3525.

(b) Synthesis of α,α-5,15-Bis(8-carboxy-1-naphthyl)-10,20-dimesitylporphyrin, 2a. A portion of 0.370 g (0.43 mmol) of the porphodimethene (**2**) was dissolved in 35 mL of THF, and 1.3 mL of a 30% aqueous KOH solution was added. The reaction mixture was refluxed for 3 h and then acidified with 10 mL of 6 N HCl. After the mixture was stirred for an additional 5 min, a mixture of 10 mL of H_2O and 30 mL of CH_2Cl_2 was added. The dark green organic layer was washed with water (3×) and dried over $NaSO_4$. The solvent was removed, and the residue was redissolved in a mixture of 15 mL of CH_2Cl_2 and 10 mL of hexanes. Slow removal of the solvents under vacuum afforded **2a** as a purple microcrystalline solid. Yield: 0.355 g (92%). UV−vis ($CHCl_3$) λ_{max}, nm: 432. ^{1}H NMR (300 MHz, $CDCl_3$): δ 8.85 (d, 2H, J = 7.2 Hz), 8.63 (d, 4H, J = 4.7 Hz), 8.61 (d, 4H, J = 4.7 Hz), 8.33 (d, 2H, J = 8.2 Hz), 8.16 (d, 2H, J = 8.2 Hz), 8.02 (dd, 2H, J_1 = 7.2, J_2 = 8.2 Hz), 7.41 (dd, 2H, J_1 = 7.2, J_2 = 8.2 Hz), 7.24 (s, 2H), 7.18 (s, 2H), 7.06 (d, 2H, J = 7.2 Hz), 2.56 (s, 6H), 2.01 (s, 6H), 1.67 (s, 6H). HRMS−FAB (*m*/*z*): MH^+ calcd for $C_{60}H_{47}N_4O_4$, 887.3597; found, 887.3595.

(c) Synthesis of α,α-5,15-Bis(8-methoxycarbonyl-1-naphthyl)-10,20-dimesitylporphyrin, 2b. A total of 50 mg (2.17 mmol) of Na was added to a mixture of 5 mL of MeOH and 10 mL of THF. After the sodium had completely reacted, a portion of 200 mg (0.23 mmol) of the porphodimethene (**2**) was added. The solution was stirred for 2 h before oxygen was bubbled through the reaction mixture. After 5 min, 15 mL of water and 35 mL of CH_2Cl_2 were added. The organic layer was separated and immediately washed with water (3×). The organic layer was dried ($NaSO_4$), and the solvents were removed under reduced pressure. Purification was achieved by column chromatography (silica, CH_2Cl_2/hexanes, 4:1). Yield: 145 mg (69%). UV−vis (CH_2Cl_2) λ_{max}, nm (log ϵ): 425 (5.67). ^{1}H NMR (300 MHz): δ 8.57 (d, 4H, J = 4.8 Hz), 8.52 (d, 4H, J = 4.8 Hz), 8.48 (d, 2H, J = 7.1 Hz), 8.31 (d, 2H, J = 8.3 Hz), 8.22 (d, 2H, J = 8.3 Hz), 7.91 (dd, 2H, J_1 = 7.1, J_2 = 8.3 Hz), 7.50 (dd, 2H, J_1 = 7.1, J_2 = 8.3 Hz), 7.23, 7.22 (br, s 6H), 2.57 (s, 6H), 1.91 (s, 6H), 1.84 (s, 6H), −0.04 (s, 6H), −2.36 (s, 2H). HRMS−FAB (*m*/*z*): MH^+ calcd for $C_{62}H_{51}N_4O_4$, 915.3910; found, 915.3946.

(d) Synthesis of α,α-5,15-Bis(8-hydoxymethyl-1-naphthyl)-10,20-dimesitylporphyrin, 2c. A portion of the porphodimethene (**2**) (122 mg, 0.14 mmol) was dissolved in 20 mL of THF, and 60 mg of $NaBH_4$ (1.58 mmol) dissolved in 2 mL of MeOH was added. After 3 min, another sample of $NaBH_4$ (50 mg, 1.32 mmol) was added to the reaction mixture, and the solution was stirred for 1 h. The mixture was treated with 20 mL of 2 N HCl followed by 30 mL of CH_2Cl_2. The organic phase was separated, washed with water (3×), and subsequently dried over anhyd Na_2SO_4. The solvents were removed under reduced pressure, and the purple residue was redissolved in 20 mL of CH_2Cl_2. After addition of 5 mL of hexanes, the CH_2Cl_2 was slowly distilled off, and the remaining light-brown hexane solution decanted from the microcrystalline material. Removal of residual hexanes under vacuum yielded analytically pure **2b**. Yield: 120 mg (98%). UV−vis (CH_2Cl_2) λ_{max}, nm (log ϵ): 424 (5.60). ^{1}H NMR (300 MHz, $CDCl_3$): δ 8.55 (d, 4H, J = 4.6 Hz), 8.47 (d, 4H, J = 4.6 Hz), 8.30 (d, 2H, J = 7.8 Hz), 8.16 (dd, 2H, J_1 = 6.5, J_2 = 3.1 Hz), 8.07 (d, 2H, J = 6.6 Hz), 7.72 (dd, 2H, J_1 = J_2 = 7.6 Hz), 7.65−7.60 (m, 4H), 7.21 (s, 4H), 3.24 (s, 4H), 2.56 (s, 6H), 1.85 (s, 6H), 1.78 (s, 6H), 0.21 (bs, 2H), −2.28 (s, 2H). HRMS−FAB (*m*/*z*): MH^+ calcd for $C_{60}H_{51}N_4O_2$, 859.4012; found, 859.4050.

(e) Synthesis of [*syn-dispiro*[2*H*-Acenaphthylen-1-one-2,5′-10′,20′-dimesityldihydroporphyrinato-15′,2″-2″*H*-acenaphthylen-1″-one]] zinc, 2d. A portion of the porphodimethene (**2**) (100 mg, 0.117 mmol) was dissolved in 25 mL of chloroform, and 2 mL of a saturated solution of $Zn(OAc)_2 \cdot 2H_2O$ in methanol was added. The reaction mixture was refluxed for 1 h, cooled to rt, and washed with water (2×). The organic phase was dried (Na_2SO_4), and removal of the solvents yielded **2d** as a reddish-brown solid. Yield: 104 mg (97%). UV−vis (CH_2Cl_2) λ_{max}, nm (log ϵ): 477 (5.13). ^{1}H NMR (300 MHz): δ 8.19 (dd, 4H, J_1 = J_2 = 7.8 Hz), 8.01 (d, 4H, J = 7.3 Hz), 7.87−7.76 (m, 4H), 6.85 (s, 2H), 6.77 (s, 2H), 6.23 (d, 4H, J = 4.1 Hz), 5.96 (d, 4H, J = 4.1 Hz), 2.27 (s, 6H), 2.22 (s, 6H), 1.92 (s, 6H). HRMS−FAB (*m*/*z*): MH^+ calcd for $C_{60}H_{43}N_4O_2Zn$, 915.2677; found, 915.2678.

(f) Synthesis of [*syn-dispiro*[2*H*-Acenaphthylen-1-one-2,5′-10′,20′-dimesityldihydroporphyrinato-15′,2″-2″*H*-acenaphthylen-1″-one]] copper, 2e. A sample of the porphodimethene (**2**) (79 mg, 0.093 mmol) was dissolved in 20 mL of $CHCl_3$, and 2 mL of a hot, saturated solution of $Cu(OAc)_2 \cdot H_2O$ in MeOH was added. The reaction mixture was heated under reflux for 1 h. After being cooled to rt, the solvents were removed, and the residue was redissolved in $CHCl_3$. The solution was filtered through a short pad of silica gel (CH_2Cl_2). Removal of the solvent yielded **2b** as a reddish-brown solid. Yield: 84 mg (99%). UV−vis ($CHCl_3$) λ_{max}, nm (log ϵ): 486 (5.08). HRMS−FAB (*m*/*z*): MH^+ calcd for $C_{60}H_{43}N_4O_2Cu$, 914.2681; found, 914.2685.

(g) Synthesis of [α,α-5,15-Bis(8-carboxy-1-naphthyl)-10,20-dimesitylporphyrinato]zinc, 2g. A portion of 220 mg (0.240 mmol) of the metalated (Zn) dimesitylporphodimethene (**2d**) was dissolved in 25 mL of THF, and 1 mL of 30% KOH(aq) was added. The mixture was refluxed for 3 h, cooled to rt, and transferred to a separatory funnel. The aqueous solution was removed, and the organic layer was acidified with 40 mL of 0.1 N aqueous HCl. A total of 80 mL of diethyl ether was added; the organic layer was separated, immediately washed with water (2×), and dried over Na_2SO_4. Removal of the solvent under reduced pressure afforded **2g** as a purple solid. Yield: 170 mg (75%). UV−vis ($CHCl_3$) λ_{max}, nm (log ϵ): 431 (5.60). ^{1}H NMR ($CDCl_3$): δ 8.85 (2H, d, J = 7.3 Hz), 8.61 (8H, s), 8.31 (2H, d, J = 8.3 Hz), 8.18 (2H, d, J = 8.3 Hz), 8.02 (2H, dd, J_1 = J_2 = 7.7 Hz), 7.40 (2H, dd, J_1 = J_2 = 7.7 Hz), 7.20 (2H, s), 7.18 (2H, s), 7.03 (2H, d, J = 7.3 Hz), 2.56 (6H, s), 1.94 (6H, s), 1.68 (6H, s). HRMS−FAB (*m*/*z*): M^+ calcd for $C_{60}H_{44}N_4O_4Zn$, 948.2654; found, 948.2677.

(h) Synthesis of α,*β*-5,15-Bis(8-carboxy-1-naphthyl)-10,20-dimesitylporphyrin Dipotassium Salt, 3a. The porphodimethene (**3**) (150 mg, 176 mmol) was reacted with 30% KOH(aq) as described for the preparation of **2a**. The dipotassium salt formed during the reaction was filtered off and washed with THF. Recrystallization was achieved by diffusion of ether to a methanolic solution of the crude product. The purple crystalline material was collected and dried in vacuo

to yield **3a** (114 mg, 65%). Anal. Calcd for $C_{60}H_{44}N_4O_4K_2$·MeOH: C, 73.62; H, 4.86; N, 5.63. Found: C, 73.22; H, 4.77; N, 5.70. UV−vis (MeOH) λ_{max}, nm: 431. ^{1}H NMR (300 MHz, CD_3OD): δ 8.54 (br, s, 4H), 8.41 (br, s, 4H), 8.26 (d, 2H, J = 8.2 Hz), 8.11 (d, 2H, J = 8.2 Hz), 7.99 (d, 2H, J = 7.1 Hz), 7.76 (dd, 2H, $J_1 = J_2$ = 7.7 Hz), 7.52 (dd, 2H, $J_1 = J_2$ = 7.6 Hz), 7.32 (d, 2H, J = 7.2 Hz), 7.21 (s, 4H), 2.53 (s, 6H), 1.85 (s, 12 Hz).

(i) Synthesis of α,β-5,15-Bis(8-methoxycarbonyl-1-naphthyl)-10,20-dimesitylporphyrin, 3b. A portion of the porphodimethene (**3**) (200 mg, 0.23 mmol) was reacted with NaOMe as described for the preparation of **2b**, with a reaction time of 1.5 h. Purification was achieved by column chromatography (silica, CH_2Cl_2/hexanes, 4:1 to CH_2Cl_2 gradient). Yield: 173 mg (81%). UV−vis ($CHCl_3$) λ_{max}, nm (log ϵ): 425 (5.53). ^{1}H NMR (300 MHz): δ 8.61 (d, 4H, J = 4.8 Hz), 8.57 (d, 4H, J = 4.8 Hz), 8.40 (d, 2H, J = 7.1 Hz), 8.34 (d, 2H, J = 8.3 Hz), 8.28 (d, 2H, J = 8.3 Hz), 7.91 (dd, 2H, J_1 = 8.3, J_2 = 7.1 Hz), 7.58 (dd, 2H, J_1= 8.3, J_2 = 7.1 Hz), 7.38 (d, 2H, J = 7.1 Hz), 7.26 (s, 4H), 2.61 (s, 6H), 1.90 (s, 12H), 0.36 (s, 6H), −2.32 (s, 2H). HRMS−FAB (*m*/*z*): MH^+ calcd for $C_{62}H_{51}N_4O_4$, 915.3910; found, 915.3909.

(j) Synthesis of α,β-5,15-Bis(8-hydroxymethyl-1-naphthyl)-10,20-dimesitylporphyrin, 3c. A portion of the porphodimethene (**3**) (108 mg, 0.127 mmol) was reacted with $NaBH_4$ as described for **2c**. Yield: 106 mg (98%). UV−vis (CH_2Cl_2) λ_{max}, (log ϵ): 424 (5.58). ^{1}H NMR (300 MHz): δ 8.58 (d, 4H, J = 4.6 Hz), 8.50 (d, 4H, J = 4.6 Hz), 8.31 (d, 2H, J = 8.2 Hz), 8.11−8.17 (m, 4H), 7.74 (dd, 2H, $J_1 = J_2$ = 7.6 Hz), 7.60−7.62 (m, 4H), 7.22 (s, 4H), 3.04 (d, 4H, J = 5.4 Hz), 2.57 (s, 6H), 1.82 (s, 12H), 0.22 (t, 2H, J = 5.7 Hz), −2.29 (s, 2H). HRMS−FAB (*m*/*z*): MH^+ calcd for $C_{60}H_{51}N_4O_2$, 859.4012; found, 859.3964.

(k) Synthesis of [*anti-dispiro*[2*H*-Acenaphthylen-1-one-2,5′-10′,20′-dimesityldihydroporphyrinato-15′,2″-2″*H*-acenaphthylen-1″-one]] zinc, 3d. The porphodimethene **(3)** (50 mg, 0.059 mmol) was treated with $Zn(OAc)_2$ as described for **2d** (1.5 h reaction time). Yield: 49 mg (91%). UV−vis (CH_2Cl_2) λ_{max}, nm (log ϵ): 475 (5.17). ^{1}H NMR (300 MHz): δ 8.19 (dd, 4H, $J_1 = J_2$ = 7.1 Hz), 8.12 (d, 2H, J = 7.1 Hz), 7.94 (d, 2H, J = 8.3 Hz), 7.83 (d, 2H, J = 7.2 Hz), 7.78 (d, 2H, J = 7.2 Hz), 6.80 (s, 4H), 6.27 (d, 4H, J = 4.2 Hz), 5.83 (d, 4H, J = 4.2 Hz), 2.26 (s, 6H), 2.05 (s, 12H). HRMS−FAB (*m*/*z*): MH^+ calcd for $C_{60}H_{43}N_4O_2Zn$, 915.2677; found, 915.2690.

(l) Synthesis of [*anti-dispiro*[2*H*-Acenaphthylen-1-one-2,5′-10′,20′-dimesityldihydroporphyrinato-15′,2″-2″*H*-acenaphthylen-1″-one]] copper, 3e. A portion of the porphodimethene (**2**) (100 mg, 0.117 mmol) was dissolved in 25 mL of $CHCl_3$, and 60 mg (0.305 mmol) of $Cu(OAc)_2$·H_2O dissolved in 5 mL of MeOH was added. The reaction mixture was refluxed for 2 h, and the solvents were subsequently removed under reduced pressure. The residue was redissolved in CH_2Cl_2 and filtered through a small pad of silica gel. Removal of the solvent afforded **3e** as a reddish-brown solid. Yield: 105 mg (98%). UV−vis ($CHCl_3$) λ_{max}, nm (log ϵ): 483 (5.09). HRMS−FAB (*m*/*z*): MH^+ calcd for $C_{60}H_{43}N_4O_2Cu$, 914.2681; found, 914.2641.

(m) Synthesis of [α,β-5,15-Bis(8-carboxy-1-naphthyl)-10,20-dimesitylporphyrinato]zinc Dipotassium Salt, 3g. The metalated (Zn) porphodimethene **3d** (220 mg, 0.240 mmol) was reacted with 2 mL of 30% KOH(aq) in 30 mL of THF as described for **3a**. The reaction mixture was refluxed for 3 h. The volume was subsequently reduced by 60%, and the precipitated porphyrin dipotassium salt was isolated by filtration. Slow addition of ether into a methanolic solution of the crude product gave **3g** (115 mg) in 46% yield as a microcrystalline solid. UV−vis (MeOH) λ_{max}, nm (log ϵ): 430 (5.63). ^{1}H NMR (MeOD): δ 8.54 (4H, d, J = 4.6 Hz), 8.42 (4H, d, J = 4.6 Hz), 8.24 (2H, d, J = 7.6 Hz), 8.17 (2H, d, J = 7.6 Hz), 8.08 (2H, d, J = 7.6 Hz), 7.78 (2H, dd, $J_1 = J_2$ = 7.6 Hz), 7.46 (2H, dd, $J_1 = J_2$ = 7.6 Hz), 7.19 (6H, m), 2.55 (6H, s), 1.87 (12H, s). Anal. Calcd for $C_{60.5}H_{44}N_4O_{4.5}K_2Zn$ (**6**·0.5MeOH): C, 69.70; H, 4.25; N, 5.37. Found: C, 69.78; H, 4.24; N, 5.40.

(n) Synthesis of [α,β-5,15-Bis(8-carboxy-1-naphthyl)-10,20-dimesitylporphyrinato]copper Dipotassium Salt, 3h. Following the procedure described for **3a**, **3e** was treated with potassium hydroxide, and the potassium salt was filtered off and washed with THF. Diffusion of ether into a saturated solution of the product in MeOH afforded **3h** as a microcrystalline solid. Yield: 61%. UV−vis (MeOH) λ_{max}, nm (log ϵ): 547 (4.20), 421 (5.28). Anal. Calcd for **3h**·MeOH ($C_{61}H_{46}N_4O_5K_2Cu$): C, 69.33; H, 4.39; N, 5.30. Found: C, 69.42; H, 4.32; N, 5.32.

Complete experimental details for **4**; **4d**; **5**−**17**; **8a**−**c**; **9a**−**c**; **10c**; **11c**,**e**,**f**,**h**; **14a**−**c**; and **15a**−**c** have been included in the Supporting Information.

Acknowledgment. We thank the Research Corporation (Research Innovation Award 0162), the Deutsche Forschungsgemeinschaft (postdoctoral fellowship for M.H.), and the University of Florida (fellowship for H.S.G.; startup funds for M.J.S.) for financial support. Support from the National Science Foundation (CAREER Award 9874966) is also gratefully acknowledged. We would also like to express our gratitude to Dr. Khalil A. Abboud, Dr. Ion Ghiviriga, Dr. Lidia Matveeva, and Dr. David H. Powell for their assistance.

Supporting Information Available: ^{1}H NMR spectra for the dipyrromethanes **1** and **2**, for all porphodimethenes (**2**−**17**) and their diamagnetic metal complexes (**2d**, **3d**, and **4d**), for the porphyrin diacids (dipotassium salts) **2a**, **8a**, **9a**, **14a**, and **15a**, and for all porphyrin dialcohols and porphyrin diesters. Complete experimental details and crystallographic data (excluding structure factors) for all compounds. This material is available free of charge via the Internet at http://pubs.acs.org.

JO010163L